

USING MULTI TEMPORAL REMOTE SENSING DATA FOR MONITORING LAND USE LAND COVER CHANGES IN EL ALAMEIN AREA, THE NORTH WESTERN COAST OF EGYPT

**Emad Fawzy Abdelaty, Ahmed Mohamed Fayed,
Ahmed Harb Rabia.**

Natural Resources and Agricultural Engineering Department, Faculty of Agriculture,
Damanhour University, Egypt.

* afrstech@gmail.com: (Ahmed. M. Fayed)

ABSTRACT

The change detection of land use land cover provides decision makers with essential information to environmental management. This study aims to assess the changes of different land use land cover classes for the Northwest coast of Egypt during the period from 2003 to 2022 using remote sensing and GIS techniques. For this purpose, two ASTER images (2003 and 2010) and two sentinel-2 images (2016 and 2022) were downloaded and used. The visual interpretation classification method was used in ArcGIS software for images classification. Ground check of image classification was elaborated by Google earth and field observations. The results indicated that the elevation ranges from zero to 151 m Above Sea Level, most of the studied area lied in the flat sloping class. The area had no dominant aspect class. The changes of land cover use, 2003 to 2022, reflected by a steady increase of agricultural and urban areas vs a continuous decrease in bare soil and carbonate rocks. The agricultural soil increased from 2.32% (1494.87 ha) to 47.47% (30616.72 ha), whereas urban areas increased from 3.45% (2223.07 ha) to 6.12% (3946.07 ha), also salt marshes increased from 0.44% (238.11 ha) to 0.74% (477.41 ha). This increase was on the count of bare soil decreasing by 51.50% and carbonate rocks by 0.76. As for, greenhouses class was not found in the study area until 2016, but it appeared in 2022 as a new project

of land reclamation (2662.89 ha). The overall accuracy evaluation was 80% for land use land cover map in 2022. Mapping of the land use land cover changes can be used to help the decision makers for urban planning and environmental management in the study area.

Keywords: Land Use Land Cover, Change Detection, Remote Sensing, GIS, ASTER, Sentinel-2, Overall Accuracy, Northwestern coast, Egypt.

<https://doi.org/10.21608/jaesj.2023.207376.1084>

INTRODUCTION

Northwestern coast of Egypt is considered one of the most promising areas for agricultural, tourist, urban, and industrial development (**Karam et al., 2020**). Therefore, The Egyptian government has adopted sustainable development policies that aimed to extending agricultural land and maximizing its production. Thus, land use land cover changes detection is an urgent need for the planning of sustainable land use (**Elzahaby et al., 2015**).

The accurate and up-to-date information of land use land cover changes is vital to understand and assess the environmental implications of such changes (**Giri et al., 2005**). While remote sensing can detect such changes (**Roy et al., 2002**). Change detection is a determination of changes in land use land cover properties of multitemporal remote sensing data. The basic principle of using remote sensing data for change detection is that the process allows for the identification of changes between two or more dates (**Chan et al., 2001; Weng, 2001; Shalaby and Tateishi 2007**).

Land use and land cover are often used interchangeably, but actual meanings of these are different. Land cover is referring to surface cover of the ground, which can be vegetation, water, urban infrastructure, bare land, or others. Land cover identification, delineation and mapping are important for monitoring studies, planning activities and resource management, globally, and it provides the basis for monitoring activities (change detection) and provides land cover information for thematic maps (**Natural Resources Canada, 2022**).

Land use refers to the purpose of using the land, such as agriculture, recreation, wildlife habitat, industry, and tourism ... etc. Land use applications include baseline mapping and frequent monitoring, as timely information is needed to understand what type of land is present and to determine year-to-year changes in land use. This knowledge will help to develop strategies that balance land conservation, conflicting uses, and development pressures (**Natural Resources Canada, 2022**).

Distinguishing the difference between land cover and land use and information that can be derived from each are important. Land properties measured by remote sensing techniques are related to land cover type, from which land use can be identified, especially with a priori knowledge (**Natural Resources Canada, 2022**).

International researchers have put considerable effort into studying how to use remotely sensed images to detect changes in land use and land cover. **Seyam et al. (2023)** used an integrated approach to identify the changing land use land cover (LULC) at Bhaluka in Mymensingh, Bangladesh. **Schaefer and Thinth (2019)** evaluated land cover change in Ho Chi Minh City, Vietnam. **Mohammed et al. (2018)** assessed land use land cover changes in Karbala City (Iraq) using GIS techniques and remote sensing data. (**Hamud et al., 2019; Norzin and Daliman 2022**) used remote sensing and GIS for mapping and monitoring land use land cover in Malaysia. In Turkey, **Ikiel, et al. (2013)** used remote sensing and GIS-based integrated analysis of land cover change in Duzce plain and its surroundings. **Sansare and Mhaske (2020)** mapped land use changes and their impact on stormwater runoff using remote sensing and GIS as a case study of Mumbai in India .

In Egypt, several researchers applied different change detection techniques to study the change in land use and land cover. **Elzahaby et al. (2015)** used supervised classification of remote sensing imagery and the calculation of normalized difference vegetation index (NDVI) as effective tools to monitor the land use and land cover changes in Burg El Arab region, Northwest coast, Egypt. **Shalaby and Tateishi (2007)** detected land use land cover changes in the Northwestern coastal zone

of Egypt using remote sensing and GIS, this is a last search done in the study area (about 15 years ago), so our study is a very vital to detect the new changes in this promising investment region. Detection of land use and land cover change in Egyptian Nile Delta using remote sensing (**Elagouz et al., 2018**). **Hegazy and Kaloop (2015)** used remote sensing and GIS techniques for monitoring urban growth and land use change detection in Daqahlia governorate, Egypt. High-spatial resolution google earth imagery and GIS techniques was used to land use change detection and prediction on ElBeheira governorate, Egypt (**Abdelaty, 2016**). **Abd El-Hameed et al. (2020)** detected land use and land cover change in Ber El-Abd area, North Sinai, Egypt using remote sensing.

This study aims to use the integration between remote sensing and geographic information systems to study changes in land use land cover and its impact on the agriculture situation during different periods (2003 – 2022) in the study area.

MATERIALS AND METHODS

The study was elaborated through five stages (Figure1):

1. Selection and Delineation of the Study Area
2. Data Collection.
3. Data Processing.
4. Field work.
5. Remote Sensing Data Processing and GIS Analysis.

In the **First Phase**, the boundary of the study area was created to determine the extent of our analysis. In the **Second Phase**, data and information were collected (survey data, maps, satellite images, google earth, etc.), input, and summarized to get a general overview of the study area. In the **Third phase**, satellite data of ASTER and sentinel-2 were used to map soil surface conditions and detect environmental changes. In the **Fourth Phase**, during the fieldwork, the main duties were done: general data collection which was necessary for the final evaluation. Some of those included information were on soils, geology, geomorphology, natural vegetation, land use and land cover. In the **Fifth and Final Phase**, remotely sensed analysis was done for mapping the topography of the land surface, and land use land cover change detection of the study area (Figure1).



Figure1 : Study Framework.

1- Study Area

The Northwest Coast of Egypt forms a belt about 20 Km deep, which extends for about 500 km between Amria (20 Km west of El-Alexandria) and El-Salloum near the borders with Libya. The study area is in eastern province with a topographically low area with no distinct relief (**Fehlberg and Stahr, 1985**). The study area is located at occupies a portion of the northwestern side of the coastal zone in western desert of Egypt. It extends from El Hammam city (E) to new El-Alamein city (W) between $30^{\circ} 41' 04''\text{N}$ to $30^{\circ}52' 33''\text{N}$ and $28^{\circ} 48' 41''\text{E}$ to $29^{\circ} 19' 21''\text{E}$ with an area of approximately 645 Km^2 (64500 ha) (Figure2).

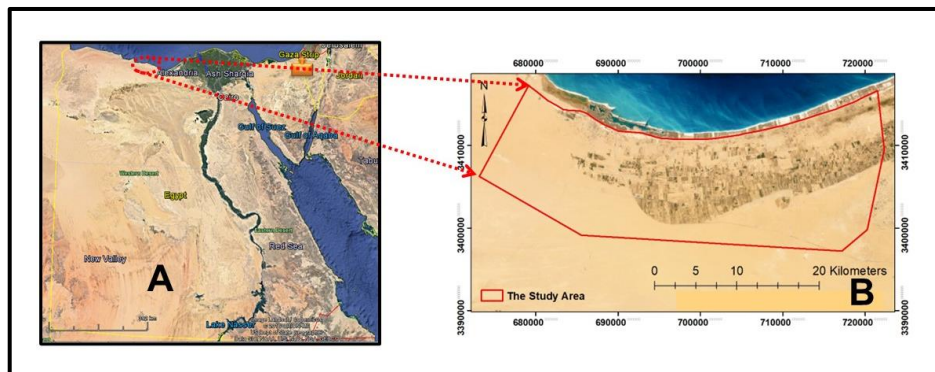


Figure2 : A- Egypt Map; B- The Study Area.

2- Data Collection

The data collection includes satellite images and maps covering the studied area. Multitemporal advanced spaceborne thermal emission and reflection radiometer (ASTER) imageries of 2003, 2010 and high-resolution cloud free sentinel-2 data of 2016, 2022 were used for mapping land use land cover classes of the study area dated 2003 to 2022 (**EarthExplorer, 2022**). ASTER and sentinel-2 datasets consist of multispectral bands out of which only three bands (VNIR) have been used for ASTER (15 m spatial resolution) and four bands (VNIR) for sentinel-2 (10 m spatial resolution) in the study, respectively (Figure3). All data projected in UTM/WGS 84, Zone 35 N.

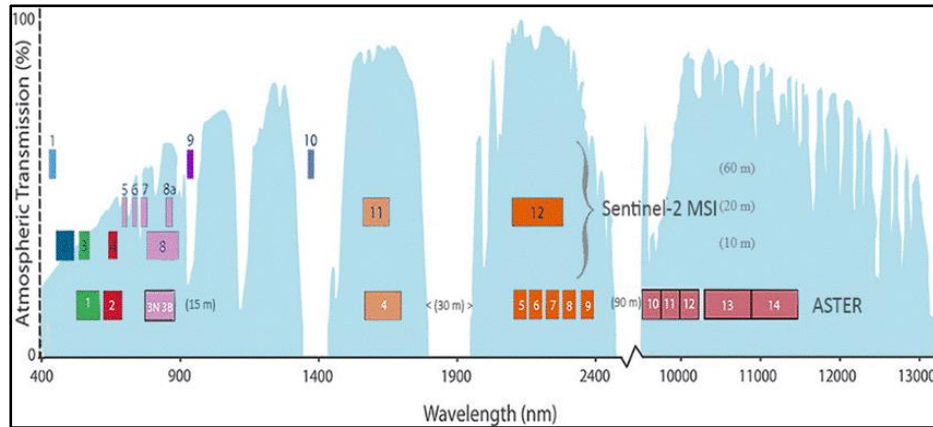


Figure3 : Comparison-bands of ASTER and Sentinel-2 sensors (Kabolzade et al., 2022).

3- Derivation of Digital Elevation Model (DEM)

DEM generation and analysis: A digital elevation model (DEM) was downloaded from earth explorer website (<https://earthexplorer.usgs.gov>, 2022). The spatial resolution is 15x15 m. This DEM was useful for a preliminary understanding of the geomorphology of the study area.

4- Derivation of Slope Gradient and Slope Aspects

Slope identifies the maximum rate of change in value from each cell to its neighbors and could be calculated as percent slope. The slope aspect identifies the down-slope direction of the maximum rate of change in value from each cell to its neighbors. Aspect can be thought of as the slope direction. The values of the output grid are the compass direction of the aspect. It is divided into 360 degrees and then grouped into eight classes centered on the compass directions (FAO, 1990). Slope gradient and slope aspects were derived from DEM using ArcMap software (ArcMap, 2011) and classified according to (FAO, 1990) as shown in (Table 1 and 2).

Table 1: Classes of Gradient Slope.

No.	Class Type	Slope	No.	Class Type	Slope
1	Flat	0.0 - 0.5	5	Moderately	10 – 15
2	Nearly	0.5 - 1	6	Strongly	15 – 30
3	Gently	1-5	7	Steep	30 – 60
4	Sloping	5 – 10	8	Very steep	> 60

Table 2: Aspect Classes and their Azimuth Ranges.

Aspect (Class)	Compass Direction	Azimuth Range (Degree)
1	North	00° – 22.5° and 337.5° – 360.0°
2	Northeast	22.5° – 67.5°
3	East	67.5° – 112.5°
4	Southeast	112.5° – 157.5°
5	South	157.5° – 202.5°
6	Southwest	202.5° – 247.5°
7	West	247.5° – 292.5°
8	Northwest	292.5° – 337.5°

5- Mapping of Land Use Land Cover

Visual interpretation (Asner et al., 2002; Slater and Brown, 2000) was done for land use land cover classification using ArcGIS 10.8 software.

6- Accuracy Assessment of Classification:

The accuracy assessment utility allows you to compare certain pixels in the thematic raster layer to reference pixels, for which the class is identified. This is an organized way of comparing your classification with ground truth data, previously tested maps, aerial photos, or other data. Different techniques were applied to assess the accuracy of classified satellite images; some of these techniques can be summarized as follows (ERDAS, 1999):

- **producer's accuracy** = $(X_{ii}/X_{i+}) \times 100$

where:

X_{ii} → number of pixels classified correctly.

X_{i+} → total number of pixels in the Referenced class,

- **User's accuracy** = $(X_{ii}/X_{i+}) \times 100$

where:

X_{ii} → number of pixels classified correctly.

X_{i+} → the total number of pixels in the classified class.

- **Overall accuracy** = $(\sum_{i=1}^k X_{ii}/N) \times 100$

where:

P_o → overall accuracy

X_{ii} → number of pixels classified correctly.

N → total number of pixels.

7- Remotely Sensed Change Detection of Land Use Land Cover:

Change detection is the process of identifying differences in the state of an object or phenomenon by observing it at different times. Essentially, it involved the ability to quantify temporal effects using multitemporal data (Singh, 1989). The visual analysis category was used for land use land cover change detection. It includes visual interpretation of multitemporal images composite and on-screen digitizing of changed areas (ArcMap, 2011).

RESULTS AND DISCUSSION

1- Terrain Features

1.1. Reclassified of Digital Elevation Model (DEM)

The digital elevation model (DEM) was downloaded (**EarthExplorer, 2022**) and reclassified (ArcGIS software). Figure 4 showed that the elevation ranges from zero to 151 m Above Sea Level (ASL). The dominant elevation classes that range from zero to 45m (ASL) occupied 72.41 % of the studied area. About 27.5 % of the region has an elevation ranging from 45 m to 151 m A.S.L. (Table 3 and Figure 4).

Table 3: Reclassified Digital Elevation Model of the Study Area.

DEM (m)	Area (ha)	Percentage (%)
0-15	17100.440	26.515
15-30	20285.220	31.453
30-45	9313.796	14.441
45-60	3910.611	6.063
60-75	4663.360	7.231
75-90	6023.973	9.340
90-105	2787.825	4.323
105-120	391.769	0.607
120-135	15.476	0.024
135-151	2.140	0.003
Total Area	64494.61	100.00

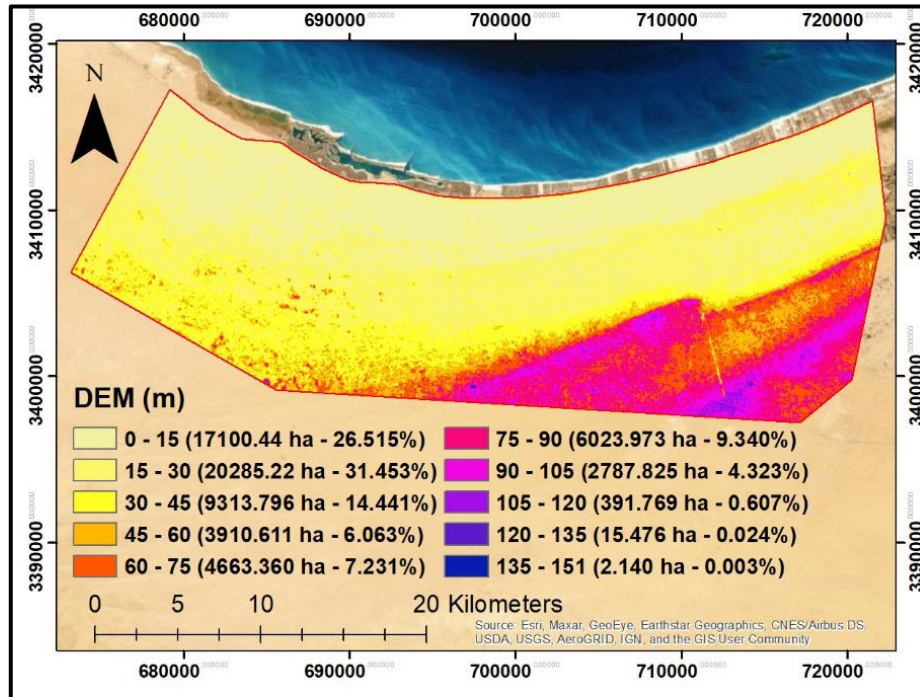


Figure 4: Reclassified Digital Elevation Model.

1.2. Slope Gradient

Slope gradients were derived from the digital elevation model (DEM) (Table 4 and Figure 5). The table showed that the studied area may be classified practically into four slope gradient classes (FAO, 1990) that range from flat slope class (0.0 - 0.15 %) to gently slope class (5.0 – 15.0 %) with an area of 63.94 % and 34.88 %, respectively. This indicated clearly that most of the studied area lies in the sloping class of flats.

Table 4: Slope Gradient Classes.

Slope	Classes	Area (ha)	Percentage (%)
0-5	Gentle to Flat	41235.03	63.94
5-15	Gentle	22496.05	34.88
15-30	Steep	753.74	1.17
>30	Very Steep	9.80	0.02
Total Area		64494.62	100.00

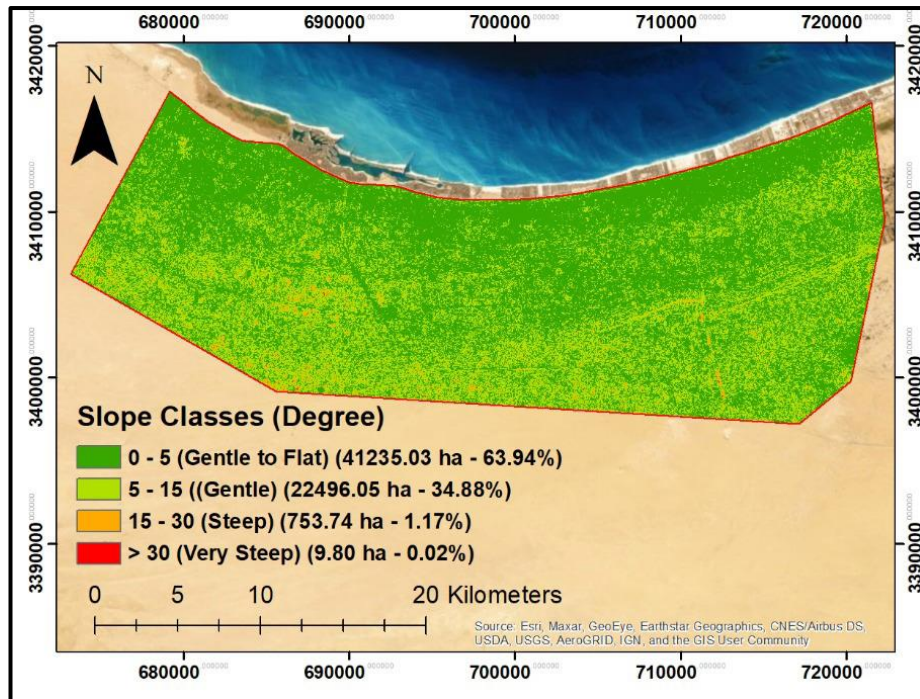


Figure5 : Slope Gradient Classes.

1.3. Slope Aspect

Aspect was interpolated from DEM to illustrate the slope direction of the studied region. The attributes aspect direction data indicated that there is no dominant class of the studied region (Table 5 and Figure 6).

Table 5: Attributed Data of Aspect Directions.

Aspect Classes	Degree	Area (ha)	Percentage (%)
Flat	-1	1172.67	1.83
North	0-22.5	4506.54	6.99
Northeast	22.5-67.5	8299.51	12.96
East	67.5-112.5	6752.03	10.54
Southeast	112.5-157.5	7434.39	11.61
South	157.5-202.5	9200.77	14.37
Southwest	202.5-247.5	7764.75	12.12
West	247.5-292.5	6861.35	10.71
Northwest	292.5-337.5	8011.55	12.51
North	337.5-360	4491.06	7.01
Total Area		64494.62	100.00

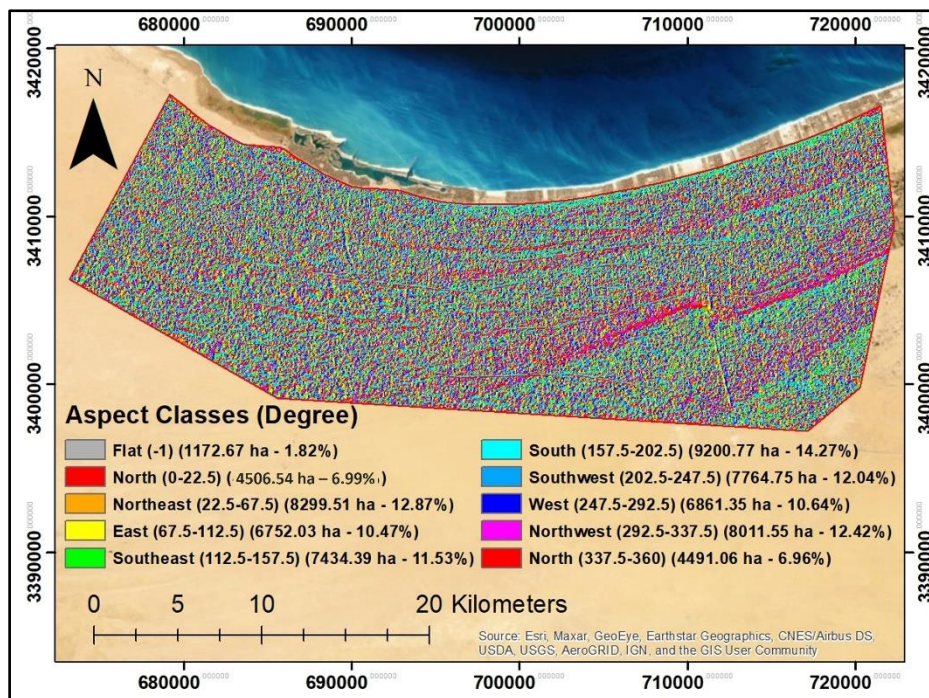


Figure6 : Slope Aspect Classes.

2- Mapping Land Use Land Cover (2022)

The visual interpretation of Sentinel-2 image dated (2022) - was elaborated by using ArcMap 10.8. The on-screen digitizing (visual interpretation) was elaborated for the multitemporal satellite images. It was based on the characters texture, shape, size, and patterns (Lu et al., 2003). This interpretation was conducted to classify the studied area into different classes of land use land cover (LULC). The relative distribution of LULC classes 2022 (Figure 11) is represented in (Table6).

Table 6: Description of Land Use Land Cover Classes.

Land Use Land Cover	Characteristics
Urban Area	Includes tourism villages along the north side of the study area and separate houses of the Bedouins.
Salt Marshes	Salt marshes are coastal wetlands that are flooded and drained by salt water brought in by the tides.
Agriculture Soil	Crop fields (annual crops, vegetables, and fruit).
Carbonate Rocks	The residue of the carbonate rocks on the soil surface.
Bare Soil	Land areas of exposed soil surface and contains sparse vegetation with very low plant cover value.
Greenhouse	A greenhouse is a structure with walls and roof made of transparent material for modify the natural environment to achieve an optimum plant growth and yields.

The LULC of the studied area that composes of five categories (2003, 2010, and 2016), and six categories (2022), and they were assessed and found to be as follows (Table7, Figures 7 - 11):

1. **Urban Area:** includes tourist buildings along the study area (summer resorts) and sporadic Bedouins houses within the local villages. Built-up areas constitute 3946.07 ha, with a percentage of about 6.12 % of the total studied area.
2. **Salt Marshes:** Salt marshes or coastal marshes are intertidal wetlands and are considered as transitional area between land and water (Shalaby and Tateishi, 2007). It is represented by a blue color on the map, and it covered 477.41 ha with an area percentage of 0.74 % of the total area.
3. **Agricultural Soil:** As shown in the map is represented by a green color. It covered 30616.72 ha of the studied area and constituted 47.47 %. It presents the biggest class in the study area.
4. **Carbonate Rocks:** The remnant of the carbonate rocks covered 225.43 ha with 0.33 % of the total studied area.
5. **Greenhouse:** This category appeared after 2016 as a result of a big governmental project for sustainable agricultural development in the study area. It covered 4.13% of the studied area, which is equivalent to 2662.89 ha.
6. **Bare Soil:** bare soil are exposed areas of soil surface, and that may be covered with sparse vegetation. It covered 26566.09 ha of the studied area and constituted 41.19 %.

Table 7: ASTER (2003 and 2010) and Sentinel-2 (2016 and 2022) Mapped Land Cover.

LULC	Satellite Data							
	ASTER				Sentinel-2			
	(2003)		(2010)		(2016)		(2022)	
	(ha)	(%)	(ha)	(%)	(ha)	(%)	(ha)	(%)
Urban Area	2223.07	3.45	2464.72	3.82	2988.66	4.63	3946.07	6.12
Salt Marshes	283.11	0.44	588.81	0.91	477.41	0.74	477.41	0.74
Agriculture Soil	1494.87	2.32	10209.04	15.83	24394.98	37.82	30616.72	47.47
Carbonate Rocks	715.79	1.11	640.36	0.99	592.84	0.92	225.43	0.35
Bare Soil	59777.77	92.69	50591.68	78.44	36040.72	55.88	26566.09	41.19
Greenhouse	0.00	0.00	0.00	0.00	0.00	0.00	2662.89	4.13
Total	64494.61	100.00	64494.61	100.00	64494.61	100.00	64494.61	100.00

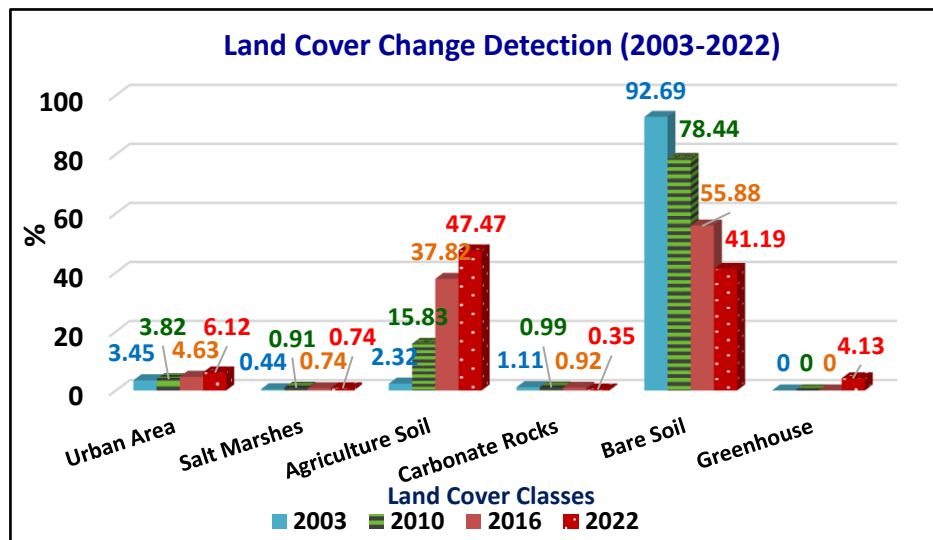


Figure7 : Comparison of land cover classes mapped by ASTER (2003 and 2010), and Sentinel-2 (2016 and 2022) satellite data.

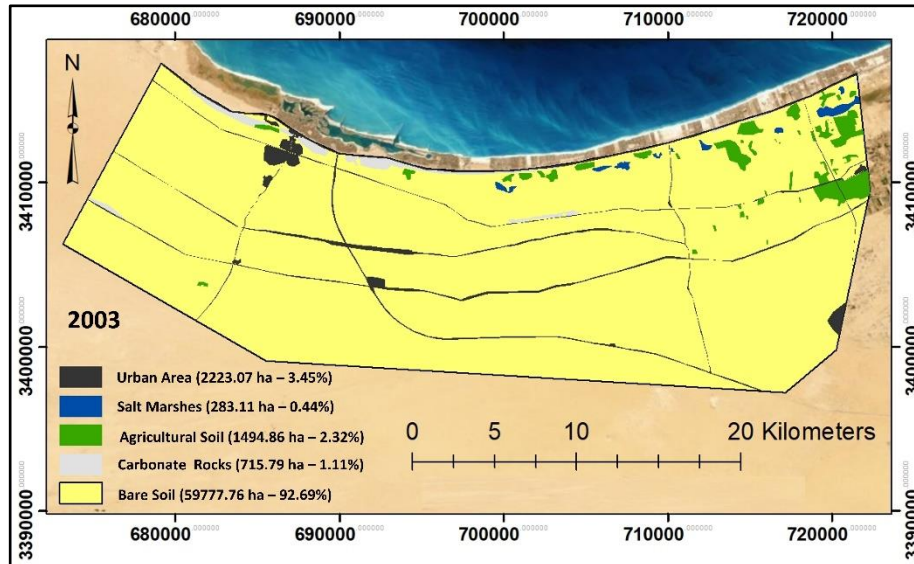


Figure 8: Land Use Land Cover 2003.

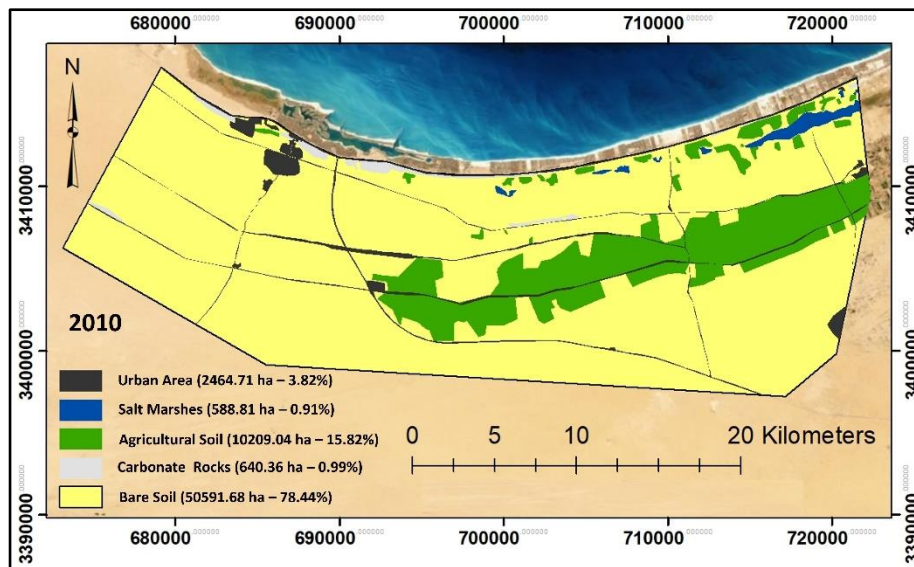


Figure 9: Land Use Land Cover 2010.

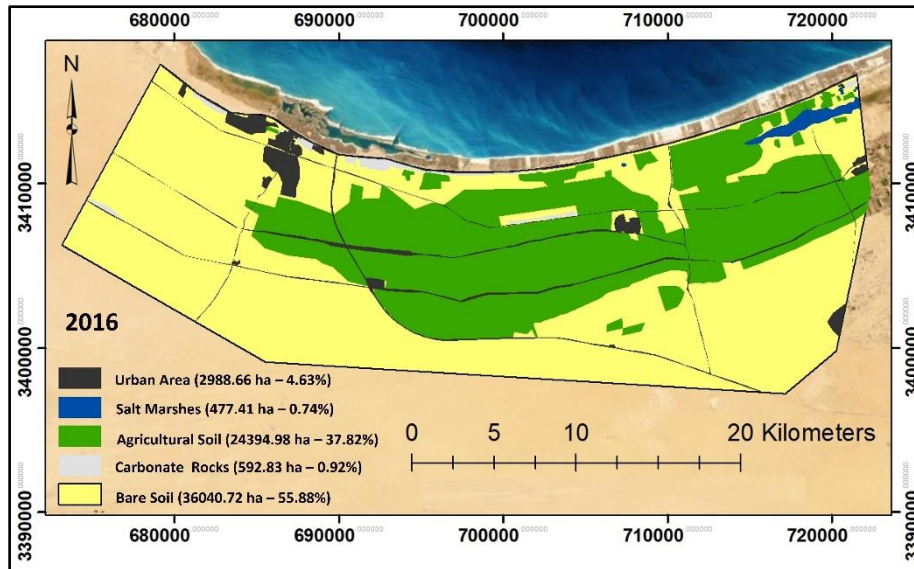


Figure10 : Land Use Land Cover 2016.

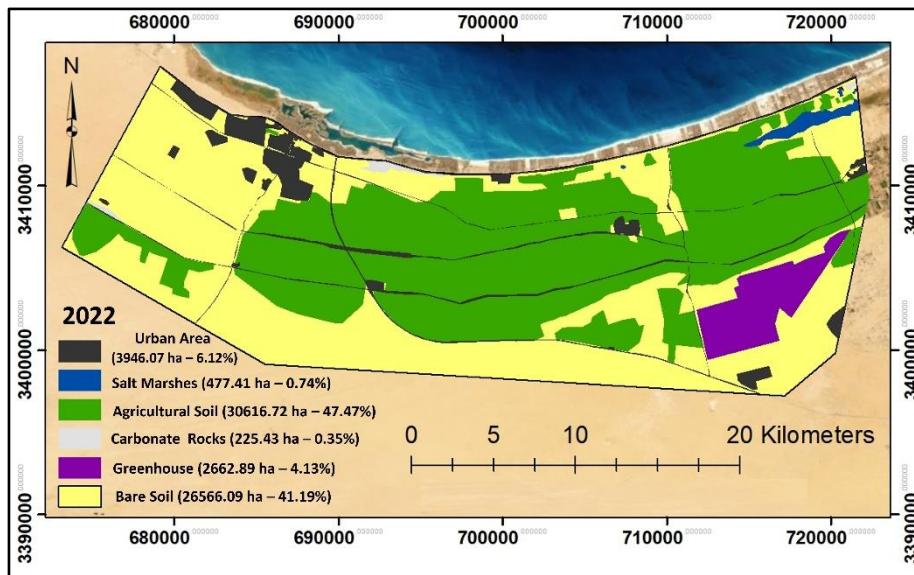


Figure11 : Land Use Land Cover 2022.

3- Accuracy Assessment of Classification (2022):

The accuracy assessment utility allows comparing certain pixels in your thematic raster layer to reference pixels. We used fifty random points for classification accuracy assessment calculating and compare between class of point and its ground reference point, such as shown in (Table8). Then the accuracy report showed in (Table9).

Table 8: Accuracy Assessment.

Point	X	Y	Reference	Class	Point	X	Y	Reference	Class
1	680988	3415346	1	1	26	710701	3401489	3	6
2	684103	3413538	1	1	27	706203	3401013	3	6
3	686752	3412415	1	1	28	696096	3401807	3	3
4	687137	3410336	1	1	29	686994	3405564	3	6
5	699962	3410386	1	1	30	680062	3404717	3	6
6	707673	3407352	1	1	31	692148	3411257	4	4
7	715418	3398383	1	1	32	692720	3411046	4	4
8	720364	3401753	1	1	33	721136	3416041	4	4
9	721487	3414812	2	2	34	675554	3408633	4	4
10	720615	3414527	2	2	35	676136	3408336	4	4
11	719660	3414225	2	2	36	720253	3406482	5	5
12	718352	3414058	2	6	37	719141	3404895	5	5
13	715503	3412585	2	6	38	717025	3404789	5	5
14	720598	3415641	2	6	39	715622	3402910	5	5
15	721531	3415793	2	2	40	712950	3400318	5	5
16	721128	3415330	3	6	41	719300	3402805	6	6
17	720433	3415171	3	3	42	712738	3403281	6	1
18	719639	3414900	3	3	43	708426	3402752	6	6
19	718025	3414576	3	3	44	709325	3409631	6	6
20	715305	3410485	3	3	45	709325	3409631	6	6
21	713717	3406887	3	3	46	695144	3409895	6	6
22	707103	3405722	3	3	47	702737	3399074	6	6
23	699800	3408633	3	3	48	692048	3400556	6	6
24	694561	3407945	3	3	49	689085	3410160	6	3
25	699641	3404823	3	3	50	679083	3409313	6	6

The overall classification accuracy was 80%, and the details of single class accuracy can be found in (Table9). This table shows that the highest procedure accuracy is for urban area, carbonate rocks, and greenhouse classes, this is due to these classes are very clear in the images. The lowest procedure accuracy was for salt marshes and agricultural soil classes. This is because the vegetation is sparse and can confuse salt marshes in satellite images.

Table 9: Accuracy Report.

Class Number	Class Name	Reference Totals	Classified Totals	Number Correct	Procedure Accuracy %	User Accuracy %	Overall Classification Accuracy %
1	Urban Area	8	9	8	100	88.89	80
2	Salt Marshes	7	4	4	57.14	100	
3	Agricultural Soil	15	11	10	66.67	90.91	
4	Carbonate Rocks	5	5	5	100	100	
5	Greenhouse	5	5	5	100	100	
6	Bare Soil	10	16	8	80	50	
Totals		50	50	40	--	--	

2.1. Change Detection of Urban Built-Up and Cultivated Area

The visual image interpretation method of multitemporal remote sensing data; ASTER (2003 and 2010), and Sentinel-2 (2016 and 2022) were used to map the land use land cover of the studied area from 2003 until 2022. ArcMap 10.8 software has allowed calculating the area and the percentage of each class. Hence, comparing each classified map with the other, it has been possible to determine the changes in land use land cover at different years from 2003 to 2022.

2.2. Analysis of Change Detection (Rate and Pattern)

This analysis was carried out to find the rate and pattern of change that had occurred. This can be achieved (for example, the period between 2003 and 2010) by subtracting the total area in 2003 from the total area in 2010, dividing the result by the total area in 2003, and multiplying the result by 100 to obtain the rate of change that occurred, which could be positive (increase) or negative (decrease) (**Abdelaty, 2016**).

The results of this study indicate drastic increasing changes in all urban areas, salt marshes, and agricultural areas in the years of the study from 2003 to 2022 and decreasing changes in the other categories. It can be observed clearly from the diagrams shown in (Figure 12) which is the outcome of temporal changes that have occurred in this duration such as urbanization and land reclamation.

The study found that in the period of the study (19 years) the urban built-up area has increased in the study area. Table (10) and (Figure12) show that: The change rate of the built-up area between 2003 and 2022 was 77.51 % (from 2223.07 ha in 2003 to 3946.07 ha in 2022). The rate of urban ratio increased in the period 2003-2010 and 2010-2016 by 10.87% and 21.26%, respectively, while increased in the period 2016-2022 by 32.03%. whereas the big change in this category was in the northwestern side of the study area as a new tourist building.

The results showed that the salt marshes exhibited different patterns of change. When the Egyptian government has paid attention to the salt marshes and worked with them as a natural environment that contain a lot of biodiversity, we find that the salt marshes have increased their area from 283.11 ha in 2003 to 588.81 ha in 2010. As a result of negative outcomes of 2011 events, it decreased after 2010 by 18.92% due to people encroaching on it. The area of the salt marshes in the study area is still stable without change from 2016 until 2022 (0.74%). The total rate of increase in the period from 2003 to 2022 was 68.63 %.

Table 10: Change Detection of Land Use Land Cover by ASTER and Sentinel-2 Data.

Land Cover Classes	Detected Change							
	2003-2010		2010-2016		2016-2022		2003-2022	
	Area(ha)	(%)	Area(ha)	(%)	Area(ha)	(%)	Area(ha)	(%)
Urban Area	241.65	10.87	523.94	21.26	957.41	32.03	1723.00	77.51
Salt Marshes	305.70	107.98	-111.40	-18.92	0.00	0.00	194.30	68.63
Agriculture Soil	8714.17	582.94	14185.90	138.95	6221.74	25.50	29121.90	1948.12
Carbonate Rocks	-75.43	-10.54	-47.52	-7.42	-367.41	-61.97	-490.36	-68.51
Greenhouse	0.00	0.00	0.00	0.00	2662.89	100.00	2662.89	100.00
Bare Soil	-9186.09	-15.37	-14551.00	-28.76	-9474.63	-26.29	-33211.70	-55.56

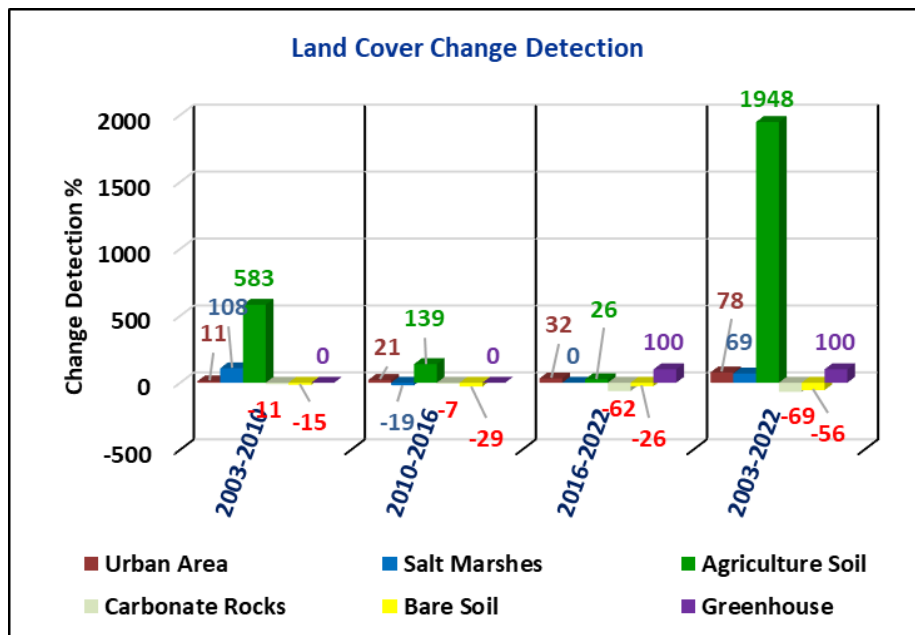


Figure12 : Land Use Land Cover Change Detection (2003 - 2022).

The efforts of the Egyptian government to ensure national food security led to the expansion of new desert land reclamation, which led to a continuous increase in the agricultural area in the study region (2003 to 2022) with a very big increase rate of 1948.12% (1494.87 hectares in 2003 to 30616.72 hectares in 2022). The record rate of changes was 582.94%, 138.95%, and 25.50% during the periods 2003-2010, 2010-2016, and 2016-2022, respectively. As well as using a specific area (2,662.61 ha) to build greenhouses for produce vegetable crops to meet the needs of the local and international market. Generally, agricultural lands in the study area are used to produce different food crops such as wheat, barley, vegetables, fig, and olive.

The interest in agricultural development in the studying area led to a decrease in the areas of both carbonate rocks (from 715.79 ha in 2003 to 225.43 ha in 2022) and uncultivated lands (from 59777.77 ha in 2003 to 26566.09 ha in 2022) with a decrease rate of 68.51 and 55.56 %, respectively.

In the end, LULC changes may either be positive or negative with corresponding impacts. In the natural context, negative conversion of LULC is the soil shift from cultivated to non-cultivated or the environment shift from rich to poor biodiversity (**Doyog et al., 2021**). For example, the positive change, in this study, is the increase in the agricultural soil, and the negative change is the decrease in the salt marshes during the period of 2010-2016.

CONCLUSION

Nowadays, change mapping of land use land is a great important for scientific, planning and management. Remote sensing satellite imagery provides an overview of the whole area in a multitemporal period. The aims of this study were detecting changes in land use land cover and its impact on the agriculture situation during different periods (2003 – 2022) in the study area using visual interpretation by the integration between remote sensing and GIS. This study showed that most of the studied area lay in the sloping class of flat and the elevation in the study area ranged from zero to 151 m Above Sea Level. The agricultural and urban areas had a continuous increase, while bare soil

and carbonate rocks had a continuous decrease in the studied area during the period from 2003 to 2022. The class of greenhouses appeared in the study area in 2022 as a new project of land reclamation. Also, it is recommended that using high resolution and updated satellite images with ground truth data in future work may help to map the land cover changes with maximum level of accuracy and this is required for quick response in decision making.

REFERENCES

- Abd El-Hameed, H. H.; Marzouk, E. R.; Abdo, M. R. and Abdelmontaleb, A. B. (2020)** Detection of land use/cover change in Ber El-Abd area, North Sinai, Egypt using remote sensing. *SINAI Journal of Applied Sciences* 9 (2) 183-190. <https://doi.org/10.21608/SINJAS.2020.36002.1002>
- Abdelaty, E. F. (2016)** Land use change detection and prediction using high-spatial resolution google earth imagery and GIS techniques: a study on ElBeheira governorate, Egypt. Fourth International Conference on Remote Sensing and Geoinformation of the Environment (RSCy2016), Proc. of SPIE Vol. 9688, 968803 · © 2016 SPIE · CCC code: 0277-786X/16/\$18 · doi: 10.1117/12.2239898.
- ArcMap 10.8. (2011)** ESRI, Environmental Systems Research Institute. U.S. copyright 2008 ESRI Inc.
- Asner, G. P.; Keller, M.; Pereira, R. and Zweede, J. C. (2002)** Remote sensing of selective logging in Amazo[^]nia—assessing limitations based on detailed field observations, Landsat ETMz, and textural analysis. *Remote Sensing of Environment*, 80: 483–496.
- Chan, J. C.; Chan, K. P. and Yeh, A. G. O. (2001)** Detecting the nature of change in an urban environment: A comparison of machine learning algorithms. *Photogrammetric engineering and remote sensing*, 67: 213-225.
- Doyog, N. D.; Lumbres, R. I. C. and Baoanan, Z. G. (2021)** Monitoring of Land Use and Land Cover Changes in Mt. Pulag

National Park Using Landsat and Sentinel Imageries. *Philippine Journal of Science*, 150 (4): 723-734.

Elagouz, M. H.; Abou-Shleel, S.M.; Belal, A. A. and El-Mohandes, M. A. O. (2018) Detection of land use and land cover change in Egyptian Nile Delta using remote sensing. *The Egyptian journal of remote sensing and space sciences*.
<https://doi.org/10.1016/j.ejrs.2018.10.004>

Elzahaby, E. M.; Suliman, A. S.; Bakr, N. and Al- Janabi, A. A. (2015) Land Cover Change Detection and Land Evaluation of Burg El Arab Region, North West Coast, Egypt. *J. Agric. Res.* Vol. 60, No.3, pp. 193-204.

ERDAS 8.4. (1999) ERDAS IMAGINE, version 8.4. ERDAS Inc., USA, 1999.

FAO (1990) Guidelines for Soil Profile Description. 3rd ed., FAO, Rome.

Fehlberg, H. and Stahr, K. (1985). Development of sustained land use by understanding soil and landscape formation in the desert fringe area of new-Egypt. *CATENA*, 12(1): 307-328.

Giri, C.; Zhu, Z. and Reed, B. (2005) A comparative analysis of the global land cover 2000 and MODIS land cover data sets. *Remote sensing of environment*, 94, 123-132.

Hamud, A. M.; Prince, H. M. and Shafri, H. Z. (2019) Landuse/Landcover mapping and monitoring using Remote sensing and GIS with environmental integration. *Sustainable Civil and Construction Engineering Conference*. IOP Conf. Series: Earth and Environmental Science, 357, 012038. doi:10.1088/1755-1315/357/1/012038

Hegazy, R. I. and Kaloop, M. R. (2015) Monitoring urban growth and land use change detection with GIS and remote sensing techniques in Daqahlia governorate, Egypt. *International journal of sustainable built environment*, 4, 117-124. <http://dx.doi.org/10.1016/j.ijsbe.2015.02.005>

EarthExplorer (2022). <https://earthexplorer.usgs.gov> (Accessed (10-01-2022)).

Natural Resource Canada (2022). <https://natural-resources.canada.ca/> (Accessed (18-02-2022)).

Ikiel, C., Ustaoglu, B.; Dutucu, A. A and Kilic, D. E. (2013) Remote sensing and GIS-based integrated analysis of land cover change in Duzce plain and its surroundings (north western Turkey).

Environ Monit Assess, 185:1699–1709 DOI 10.1007/s10661-012-2661-6

- Kabolizade, Mostafa; Rangzan, Kazem; Mousavi, Seyyed and Azhdari, Ehsan. (2022)** Applying optimum fusion method to improve lithological mapping of sedimentary rocks using sentinel-2 and ASTER satellite images. *Earth Science Informatics*. 15. 10.1007/s12145-022-00836-1.
- Karam, M. A.; Hegazi, A. M. and Seleem, T. A. (2020)** Geotechnical Evaluation of Soil at El-Alamein New City, Northern Coast, Egypt. *Journal of Petroleum and Mining Engineering* 22(1). DOI: 10.21608/jpme.2020.23635.1026.
- Lu, D.; Mausel, P.; Brondizio, E. and Moran, E. (2003)** Change detection techniques. *INT. J. REMOTE SENSING*, 2003, VOL. 25, NO. 12, 2365–2407. DOI: 10.1080/0143116031000139863
- Mohammed, E. A.; Hani, Z. Y. and Kadhim, G. Q. (2018)** Assessing land cover/use changes in Karbala city (Iraq) using GIS techniques and remote sensing data. *The Sixth Scientific Conference “Renewable Energy and its Applications”*, IOP Conf. Series: Journal of Physics: Conf. Series 1032 (2018) 012047. doi:10.1088/1742-6596/1032/1/012047
- Norzin, A. F. and Daliman, S. (2022)** Assessing Land Use and Land Cover Change Analysis Using Remote Sensing In Kota Bharu, Kelantan. *4th International Conference on Tropical Resources and Sustainable Sciences 2022*, IOP Conf. Series: Earth and Environmental Science 1102 (2022) 012079. doi:10.1088/1755-1315/1102/1/012079
- Roy, D. P.; Lewis, P. E. and Justice, C. O. (2002)** Burned area mapping using multi-temporal moderate spatial resolution data – a bi-directional reflectance model-based expectation approach. *Remote sensing of environment*, 83: 263-286.
- Sansare, D. A. and Mhaske, S. Y. (2020)** Land use change mapping and its impact on storm water runoff using Remote sensing and GIS: a case study of Mumbai, India. *The Fifth International Conferences of Indonesian Society for Remote Sensing*, IOP Conf. Series: Earth and Environmental Science, 500, 012082. doi:10.1088/1755-1315/500/1/012082
- Schaefer, M. and Thinth, N. X. (2019)** Evaluation of land cover change and agricultural protection sites: a GIS and remote sensing

approach for Ho Chi Minh city, Vietnam. *Heliyon*, 5, 01773.
<https://doi.org/10.1016/j.heliyon.2019.e01773>

Seyam, M. M. H.; Haque, M. R. and Rahman, M. M. (2023) Identifying the land use land cover (LULC) changes using remote sensing and GIS approach: A case study at Bhaluka in Mymensingh, Bangladesh. *Case Studies in Chemical and Environmental Engineering*, 7, 100293.
<https://doi.org/10.1016/j.cscee.2022.100293>.

Shalaby, A. and Tateishi, R. (2007) Remote sensing and GIS for mapping and monitoring land cover and land use changes in the Northwestern coastal zone of Egypt. *Applied Geography*, 27: 28-41. doi:10.1016/j.apgeog.2006.09.004

Singh, A. (1989) Digital change detection techniques using remotely sensed data. *International journal of remote sensing*, 10: 989-1003.

SLATER, J. and BROWN, R. (2000) Changing landscapes: monitoring environmentally sensitive areas using satellite imagery. *International Journal of Remote Sensing*, 21: 2753–2767.

Weng, Q. (2001) Land use change analysis in the Zhujiang Delta of China using satellite remote sensing, GIS and stochastic modeling. *J. Environ. Manage.* 64: 273–284.

الملخص العربي

استخدام بيانات الاستشعار عن بعد متعددة الفترات الزمنية لرصد التغيرات في استخدامات الغطاء الأرضي في منطقة العلمين، الساحل الشمالي الغربي لمصر.

عماد فوزي عبد العاطي - أحمد محمد فايد - أحمد حرب ربيع

¹قسم الموارد الطبيعية والهندسة الزراعية، كلية الزراعة، جامعة دمنهور، دمنهور، مصر

* afrstech@gmail.com: (Ahmed. M. Fayed)

يوفر الكشف عن التغييرات في استخدام الأراضي والغطاء الأرضي معلومات أساسية للإدارة البيئية، وهو مهم جدًا لصناع القرار. تهدف هذه الدراسة إلى تقييم التغيرات في فئات الغطاء الأرضي لاستخدامات مختلفة في الساحل الشمالي الغربي لمصر خلال الفترة من 2003 إلى 2022 باستخدام تقنيات الاستشعار عن بعد ونظم المعلومات الجغرافية. لتحقيق هذا الغرض، تم تنزيل صورتين من النوع ASTER (2003 و 2010) وصورتين من النوع Sentinel-2 (2016 و 2022) واستخدامها لاكتشاف تغييرات الغطاء الأرضي لاستخدام الأراضي. تم استخدام طريقة تصنيف التفسير المرئي في برنامج ArcGIS لتصنيف الصور، ثم تم استخدام Google Earth والملاحظات الميدانية لجمع النقاط العشوائية المستخدمة للتحقق من تصنيف الصور. تم التحقق من دقة تصنيف الصورة باستخدام طريقة مصفوفة الارتباك وكان تقييم الدقة الإجمالي 80% لخريطة الغطاء الأرضي للاستخدامات الأرضية في عام 2023. أشارت النتائج إلى أن ارتفاعات سطح الأرض تتراوح من صفر إلى 151 مترًا فوق مستوى سطح البحر، وتقع معظم المنطقة المدروسة في فئة السطح المسطح، ولا توجد فئة سائدة في المنطقة المدروسة حسب فئات اتجاه الميول. تم الكشف عن زيادة مستمرة في المناطق الزراعية والعمرائية وانخفاض مستمر في التربة المكشوفة وصخور الكربونات في منطقة الدراسة خلال الفترة من 2003 إلى 2022. لم يتم العثور على فئة الصوبات الزراعية في منطقة الدراسة حتى عام 2016، لكنها ظهرت في عام 2022 كمشروع استصلاح أراضي جديد بمساحة (2662.89 هكتار). زادت التربة الزراعية من 2.32% (1494.87 هكتار) إلى 47.47% (30616.72 هكتار)، في حين زادت المناطق الحضرية من 3.45% (2223.07 هكتار) إلى 6.12% (3946.07 هكتار)، كما زادت المستنقعات المالحة من 0.44% (238.11 هكتار) إلى 0.74% (477.41 هكتار). انخفضت التربة العارية من 92.69% (59777.77 هكتار) إلى 41.19% (26566.09 هكتار)، بينما انخفضت صخور الكربونات من 1.11% (715.79 هكتار) إلى 0.35% (225.43 هكتار). يمكن استخدام خرائط تغييرات الغطاء الأرضي لاستخدام الأراضي لمساعدة صانعي القرار في التخطيط الحضري والإدارة البيئية في منطقة الدراسة.